

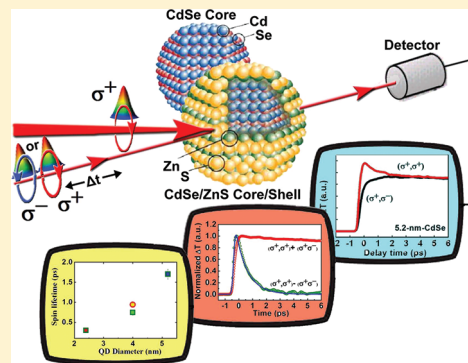
Exciton Spin Relaxation in Colloidal CdSe Quantum Dots at Room Temperature

Hong Ma,^{†,‡} Zuanming Jin,[†] Zhengbing Zhang,[†] Gaofang Li,[†] and Guohong Ma^{*,†}

[†]Department of Physics, Shanghai University, 99 Shanghai Road, Shanghai 200444, P. R. China

[‡]College of Physics and Electronics, Shandong Normal University, Jinan 250014, P. R. China

ABSTRACT: Size dependence of spin dynamics in colloidal CdSe quantum dots (QDs) are investigated with circularly polarized pump–probe transmission spectroscopy at room temperature. The excitation energy is tuned to resonance with the lowest exciton ($1S_h1S_e$) energy of the CdSe QDs. The exciton spin dynamics of CdSe QD with the diameter of 5.2 nm shows monoexponential decay with a typical time constant of about 1–3 ps depending on the excitation energy. For the cases of CdSe QDs with smaller size (with the diameter of 4.0 and 2.4 nm), the exciton spin relaxation shows biexponential decay, a fast component with time constant of several ps and a slow one with time constant of hundreds of ps to nanosecond time scale. The fast spin relaxation arises from the bright-dark transition, i.e., $J = \pm 1 \leftrightarrow \mp 2$ transition. This process is dominated by the hole spin flips, while the electron spin conserves. The slow spin relaxation is attributed to the intralevel exciton transitions ($J = \pm 1 \leftrightarrow \mp 1$ transition), which is relevant to the electron spin flip. Our results indicate that the exciton spin relaxation pathways in CdSe QD are controllable by monitoring the particle size, and polarized pump–probe spectroscopy is proved to be a sensitive method to probe the exciton transition among the fine structures.



1. INTRODUCTION

Spin-dependent effects in semiconductor quantum dots (QDs) have attracted more and more attention in recent years due to the high potential applications in spintronic devices and quantum computation.^{1–4} Spin relaxation processes are greatly suppressed by quantum confinement in all three dimensions, and spin relaxation lifetime as well as spin coherence time can be tackled by monitoring the size of semiconductor QDs.^{4–6} It has been shown that, in the quantum confinement regime, spin relaxation can exhibit very long time in comparison with the bulk counterpart.³ The most often investigated self-assembled QDs are usually strained and have an asymmetry in shape. With reducing the symmetry of QD, the degenerate two bright exciton states are mixed and split into two singlet states $|X\rangle = (|+1\rangle + |-1\rangle)/\sqrt{2}$ and $|Y\rangle = (|+1\rangle - |-1\rangle)/\sqrt{2}$ optical active in mutually orthogonal linear polarizations. As a result, the optical properties of asymmetric QDs differ substantially from those of spherically symmetrical QDs. The chemically synthesized colloidal QDs have nearly spherical shape and retain a higher symmetry. Consequently, the two bright exciton states $| \pm 1 \rangle$ are degenerate eigenstates of the Hamiltonian. Thanks to the well-developed fabricating technique, CdSe colloidal QDs with very narrow size distribution, nearly spherical shape and high quality surface passivation are available at present.^{7,8} The size-tunable carrier properties in CdSe nanocrystals were well studied in the past several decades.^{9–13} The spin dynamics in colloidal QDs^{14,15} have been much less frequently studied than that of the self-assembled QDs^{16–20} due to the random orientation of the nanocrystal in solution or

film, but it has been demonstrated that the random orientation of colloidal QDs can be partially overcome by appropriate application of nonlinear coherent spectroscopy.^{21,22} With the femtosecond time-resolved Faraday rotation (TRFR) method, spin relaxation time of CdSe QDs embedded in a transparent dielectric was determined to range from hundreds of picosecond up to nanoseconds.⁵ However, on the basis of the crossed polarized transient grating (CPTG) method that they developed recently, Scholes et al.^{23–26} demonstrated that the exciton spin relaxation time in CdSe QDs solution falls in a few picosecond and even subpicosecond time scale depending on the size of the nanocrystal. Obviously, the 2–3 orders of the difference spin lifetime measured from the TRFR and CPTG indicate that each method is only sensitive to the spin relaxation of the particular carrier. Up to now, there is no report that the individual method can identify the two very different spin relaxation times to our knowledge.

When the size of a QD is comparable or smaller than the exciton Bohr radius, the three-dimensional (3D) confinement of electron and hole results in the quantization of their states.⁹ Owing to the electron–hole exchange interaction and the crystal field, these quantization states are mixed to form an exciton fine structure in CdSe QDs.²⁷ According to calculations, the fine structure of CdSe consists of eight states, five of which are optically active (bright exciton), three of which

Received: December 5, 2011

Revised: February 2, 2012

are optically passive (dark exciton).²⁷ Exciton spin relaxation can be understood as the exciton interlevel or intralevel transitions among the exciton fine structures.²⁸ However, the characterization of the spin relaxation mechanism in QDs is still an open subject. Previous studies of exciton spin dynamics in quantum wells revealed that there are two predominant mechanisms to mediate the exciton spin relaxation:²⁹ one is a direct (or say single-step) spin flip between the $J = \pm 1$ exciton states;²⁹ the other is indirect spin flip, in which electron and hole flip their spin independently.²⁸ It is usually thought that the direct spin flip process is driven by the long-range term of the electron–hole exchange interaction,³⁰ and the indirect spin flip is governed by strong spin–orbit coupling in QDs.²⁹ In this study, we employ the circularly polarized pump–probe method to investigate the size dependence of spin relaxation in CdSe colloidal QDs. The experimental results reveal that the exciton spin relaxation of a large CdSe QD ($d = 5.2$ nm) shows monoexponential decay with a typical time constant of about 2 ps, and the smaller ones (with the diameter of 4 and 2.4 nm) show biexponential spin relaxation: a few picoseconds fast relaxation component and a hundreds of a picosecond to nanosecond slow component, the fast relaxation is believed to come from the exciton interlevel transition in which hole spin is flipped and electron spin is conserved; The slow one can be attributed to the exciton intralevel transition with the electron spin flip in the QDs. Our experimental results demonstrate that the circularly polarized pump–probe method is a sensitive method to investigate the exciton spin dynamics in colloidal QDs and also provides some insight into the exciton transition among the exciton fine structures at room temperature.

2. EXPERIMENTAL SECTION

The samples studied in this work are ensembles of CdSe QDs consisting of a CdSe core (with diameter $d = 5.2$, 4.0, and 2.4 nm) and CdSe/ZnS core/shell (with $d = 4.0$ nm) colloidal QDs solution in toluene, which were purchased from Evident Technology. Both CdSe and CdSe/ZnS QDs have wurtzite structure. High resolution TEM images revealed that all CdSe QDs have quasispherical shape with size distribution of less than 5%. During the optical orientation study, the samples were filled in a 1 mm thick glass cell. We checked the absorbance before and after optical experiment, and no absorption change was observed for all samples. The spin dynamics of the QDs solution in toluene are examined with a circularly polarized pump–probe setup at room temperature.^{31,32} Optical pulses are delivered from an Optical Parametric Amplifier (Topas-C) pumped by a Ti:sapphire laser (Spitfire Pro, Spectra-Physics) in which the output wavelength is tunable from 450 to 700 nm, with a pulse duration of 120 fs (the pulse spectra width is determined to be about 9 nm at fwhm) and a repetition rate of 1 kHz. The polarizations of both pump and probe beams can be adjusted individually by two achromatic quarter wave plates. Both pulses are focused on the sample with a spot diameter of about 200 μm for the pump and somewhat smaller for the probe beam. The transmitted probe beam is detected by a photodiode connected with a lock-in amplifier. All experiments are conducted at room temperature.

3. RESULTS

Figure 1 shows the normalized absorption spectra for both CdSe and CdSe/ZnS QDs in toluene solutions. It is seen that the lowest 1S–1S absorption peaks show blue shift with

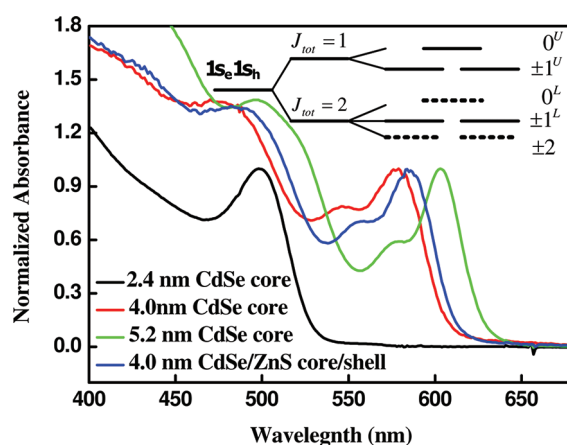


Figure 1. UV–vis absorption spectra for CdSe QDs in toluene solution, the absorbance are normalized to the lowest exciton absorption peak (1S–1S transition); the inset shows schematically the fine structure of the lowest excitonic state in QDs.

decreasing the size of QDs, e.g., the absorption peaks are at 604, 578, and 498 nm for 5.2, 4.0, and 2.4 nm CdSe core dots, and 585 nm for 4.0 nm CdSe/ZnS core–shell QDs, respectively. In the polarized pump–probe experiment, the photon energy of pump laser pulses is tuned to resonance or slightly lower to the 1S–1S exciton peak in the case of excitation of the high energy exciton states.

Figure 2a shows the transient transmission spectra of 5.2 nm CdSe core QDs under excitation of 610 nm. The curves labeled as (σ^+, σ^+) and (σ^+, σ^-) are the transmission changes obtained from cocircularly and counter-circularly polarized pump–probe beams, respectively. It is seen that a dramatic increase in transmission change occurs due to band bleaching and follows by a long recovery process. It is obvious that the amplitude of the curve (σ^+, σ^+) is much stronger than that of the curve (σ^+, σ^-) around zero delay time. Finally, both (σ^+, σ^+) and (σ^+, σ^-) curves tend to completely coincide with each other, which indicates spin polarization relaxation in the conduction band. The sum (red hollow circle) and difference (green hollow triangle) transient response are presented in Figure 2b. The sum of the two curves of (σ^+, σ^+) and (σ^+, σ^-) gives the spin-insensitive carrier dynamics, and the spin sensitive relaxation dynamic can be obtained by the difference between (σ^+, σ^+) and (σ^+, σ^-) . Here, we concentrate on the difference spectrum, which is associated with the exciton spin relaxation. It is seen from Figure 2b that the difference can be well reproduced using a single exponential decay (blue solid line). Recalling that $\tau_s/2 = \tau_{\text{flv}}$ the spin relaxation time can be determined.³¹ With increasing pump fluence, it is found that the spin relaxation time decreases from 1.80 ps at 31.8 $\mu\text{J}/\text{cm}^2$ to about 0.8 ps at 955.4 $\mu\text{J}/\text{cm}^2$. When pump fluence is higher than 1600 $\mu\text{J}/\text{cm}^2$, the two curves, (σ^+, σ^+) and (σ^+, σ^-) , show no difference, and the spin relaxation process is covered completely by the carrier relaxation. Figure 2c shows the pump fluence dependence of spin relaxation time in CdSe core QD solution at room temperature. It is seen that the spin relaxation time remains a constant value of ~ 1.8 ps when pump fluence is lower than 250 $\mu\text{J}/\text{cm}^2$, while the spin relaxation decreases rapidly with higher pump fluence. Pump fluence at 250 $\mu\text{J}/\text{cm}^2$ can be treated as the threshold value; when pump fluence is lower than that value, our calculation shows that the number of photogenerated exciton in one CdSe QD is much less than 1. The pump fluence

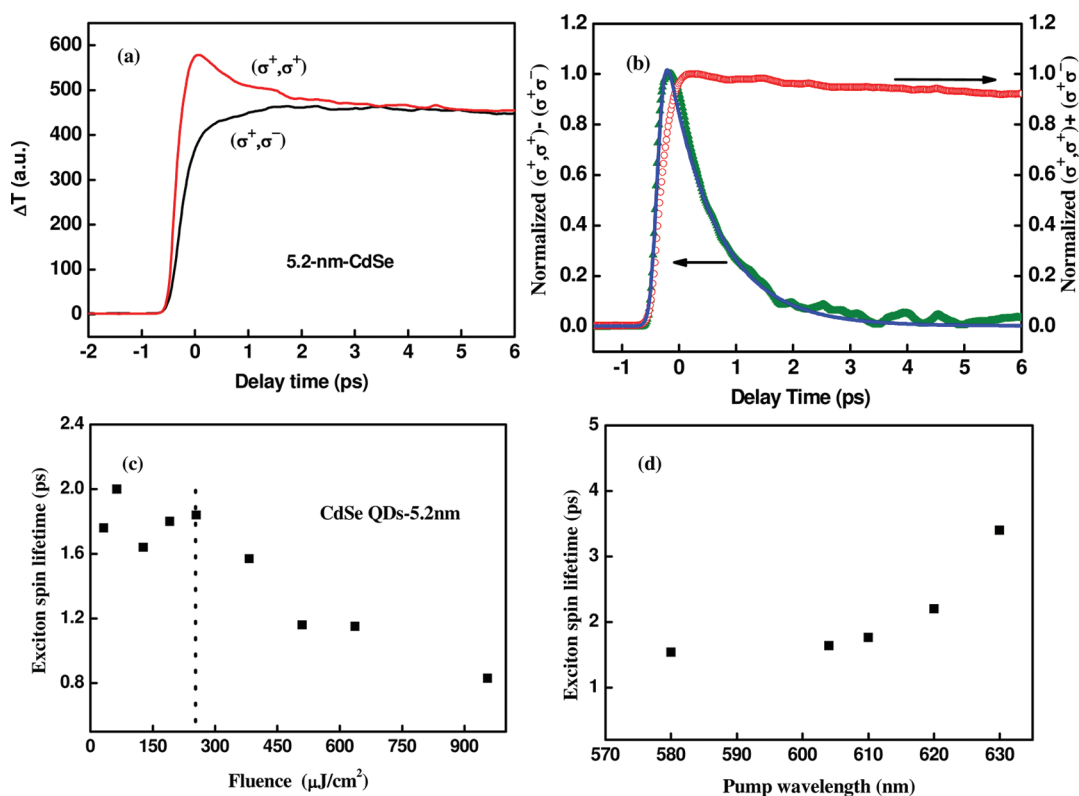


Figure 2. (a) Transient transmission change ΔT measured in 5.2 nm CdSe core QDs with the cocircularly (σ^+, σ^+) and counter-circularly (σ^+, σ^-) polarized pump–probe beams; the excitation wavelength and the pump pulse fluence are 610 nm and 190 $\mu\text{J}/\text{cm}^2$, respectively. (b) Normalized dynamics of sum $[(\sigma^+, \sigma^+) + (\sigma^+, \sigma^-)]$ and difference $[(\sigma^+, \sigma^+) - (\sigma^+, \sigma^-)]$ from the calculation of panel a; the single exponential fit is also plotted with a solid line. (c) Pump fluence dependence of exciton spin relaxation time in 5.2 nm CdSe core QD. (d) Pump energy dependence of exciton spin relaxation time in 5.2 nm CdSe QD.

remained lower than 250 $\mu\text{J}/\text{cm}^2$ for all experiments in this study in the cases of the many-body and Auger effects.

By tuning the pump wavelength from 580 to 620 nm (across the 1S–1S exciton peak), as shown in Figure 2d, the spin relaxation time does not change very much, but the trend is clearly seen that the spin relaxation time increases with pump wavelength. In general, the weak wavelength dependence of spin relaxation time can be understood as the selective excitation of QDs with particular size, the longer (shorter) pumping wavelength can selectively excite the ensemble of QDs with larger (smaller) size because the size distribution in present CdSe QDs is much larger than the spectra width of a femtosecond laser pulse, but it should be noted that if the pump wavelength is longer than 630 nm, a sharp dip around zero delay time occurs due to the two photon absorption. However, if the pump wavelength is shorter than 580 nm, the spin relaxation time decreases sharply, which may be due to the partial involvement of light-hole and the spin–orbit split-off band transitions. The experimental results demonstrate qualitatively that the spin lifetime is longer for a larger QD size.

Figure 3 shows the time dependent transmission response of 4.0 nm and 2.4 nm CdSe core QDs with resonant wavelengths of 578 and 498 nm, respectively. It is seen that the two curves, (σ^+, σ^+) and (σ^+, σ^-) , do not tend to coincide with each other up to 1 ns time scale (as shown in Figure 3b), which is significantly different from the case of 5.2 nm CdSe core QDs. The difference of two curves between (σ^+, σ^+) and (σ^+, σ^-) can be well-fitted with biexponential decay with time constants of $\tau_{\text{fit1}} = \tau_{s1}/2 = 0.37$ ps, $\tau_{\text{fit2}} = \tau_{s2}/2 > 500$ ps for 4.0 nm CdSe core QDs, and $\tau_{\text{fit1}} = \tau_{s1}/2 = 0.15$ ps, $\tau_{\text{fit2}} = \tau_{s2}/2 > 500$ ps for

2.4 nm CdSe core QDs, which are presented in Figure 3a,c, respectively. Because of the limited length of the optical delay line (~ 1 ns), we can only estimate that the relaxation time of the slow components are longer than 1 ns for both QDs. It is obtained that the *lifetime* of the *fast component* increases with QD size, and the *amplitude* of the *slow component* increases when particle size decreases, which can be seen from the Figure 2b, as well as from the insets of Figure 3a,c. These results reveal that the fast component dominates the spin relaxation process in larger size QDs, and the slow component plays a more and more important role with decreasing particle size. For example, the amplitude of the slow component for a 5.2 nm CdSe QD is almost zero, but in the case of the 2.4 nm CdSe QD, the amplitude for the slow component can reach about 50% to the whole curve.

In order to rule out the influence of surface passivation on the spin relaxation, we also studied the spin dynamics for a CdSe/ZnS core/shell structure with particle diameter of 4.0 nm. After epitaxial growth of a few layers of ZnS on the surface of the CdSe nanocrystal, the CdSe/ZnS core–shell structure is formed with good surface passivation. The surface passivation can affect the radiative lifetime, the time-resolved photoluminescence spectra revealed that the 4.0 nm CdSe core shows a 20 ns radiative decay, while radiative lifetime of 4.0 nm CdSe/ZnS core–shell structure is more than 60 ns.³³ Figure 3d presents the transient transmission spectra of 4.0 nm CdSe/ZnS core–shell QDs under excitation of 585 nm, which is corresponding to the absorption peak of the lowest exciton transition. Compared with the data obtained from CdSe core (as shown in Figure 3a), the spin relaxation of both core and

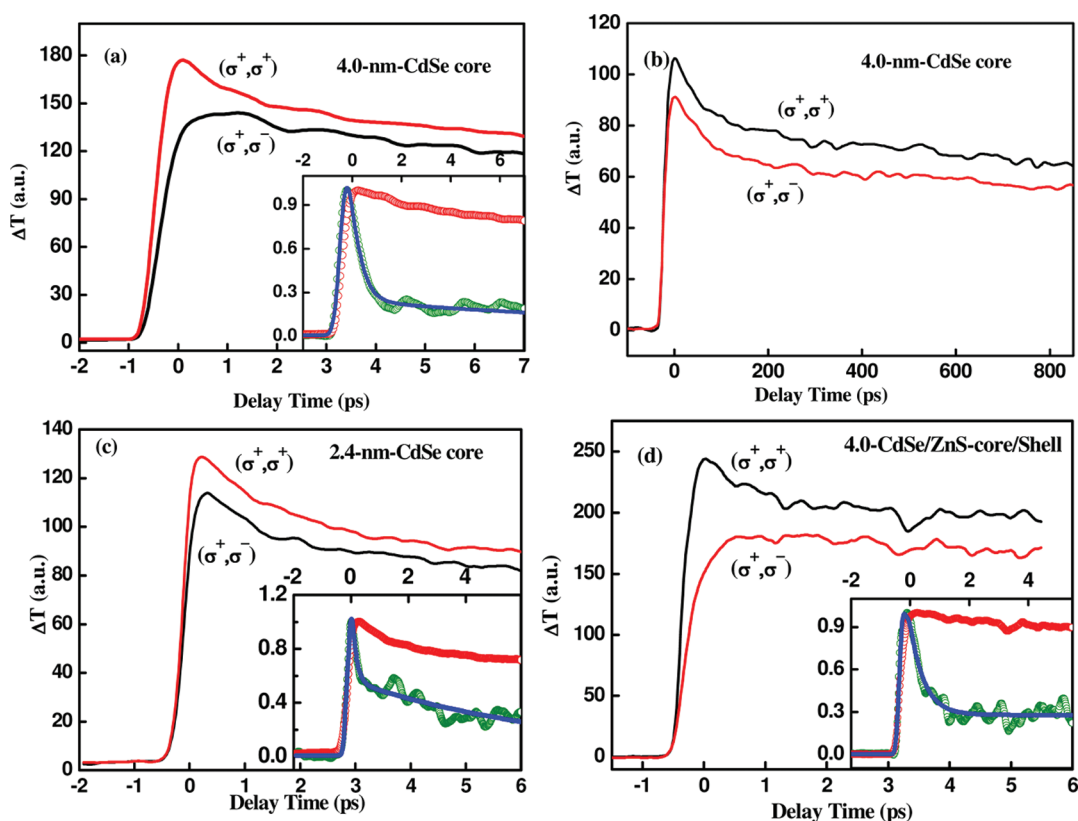


Figure 3. Transient transmission change ΔT measured in 4.0 nm (a) and 2.4 nm (c) CdSe core and 4.0 nm CdSe/ZnS core-shell (d) QDs with the cocircularly (σ^+ , σ^+) and counter-circularly (σ^+ , σ^-) polarized pump-probe beams, respectively. The central excitation wavelengths are 578 nm and 498 nm for 4.0 nm and 2.4 nm CdSe core QDs, and 585 nm for 4.0 nm CdSe/ZnS core-shell QDs, respectively. The insets in panels a, c, and d show the calculated sum and difference between (σ^+ , σ^+) and (σ^+ , σ^-) curves, and panel b shows the dynamics of ΔT for a 4.0 nm CdSe core with co- and counter-circularly polarized pump-probe beams in the long time scale. It is seen that the two curves do not coincide up to 1 ns time scale, and a similar tendency was also observed for the other two samples.

core-shell structures show biexponential decay, a fast one with a time constant of several picoseconds and slow one with hundreds of picosecond relaxation. This result indicates that surface passivated with the ZnS shell does not affect the spin dynamics significantly. The size dependence of spin lifetime shown in Figures 2 and 3 reveals that quantum confinement plays a dominate role for the exciton spin relaxation process.

4. DISCUSSION

Photoexcitation of a strongly confined QD system, such as CdSe, results in the formation of excitons. The optical properties of an exciton can be described in terms of single excitation configurations associated with transitions from a 4-fold degenerate valence band to a 2-fold degenerate conduction band.²⁶ Owing to the electron-hole exchange interaction, the mixtures of these configurations lead to the formation of the exciton fine structure. The strong spin-orbit coupling in CdSe leads to the fact that the states in the QD fine structure are not eigenstates of spin, and the total angular momentum is a good quantum number.^{26,34} As a result, the band-edge of exciton fine structure states are labeled by the total projected angular momentum, J , which is a combination of the spin and orbital angular momentum and is defined as the spin of an exciton. Previous theoretical studies of CdSe QD in the framework of 4-band $\mathbf{k}\cdot\mathbf{p}$ model revealed that the mixing between the heavy-hole and light-hole bands as well as the spin-orbit split-off bands can be neglected due to the strain induced by a large spin-orbit splitting between the heavy- and the light-hole in

strong confined CdSe QDs²⁶ (the spin-orbit splitting energy is about 420 meV for bulk CdSe). Therefore, the 8-fold degenerate lowest energy state level can be labeled as $(1S_e, 1S_h)_{S_z, F_z}$ with $S_z = \pm 1/2$, and $F_z = \pm 3/2$. The lowest excitonic state, $(1S_e, 1S_h)_{S_z, F_z}$ of CdSe QDs consists of eight fine structure states, two with $J = \pm 2$ (with $J = S_z + F_z$), four with $J = \pm 1$ and two with $J = 0$.²² Since a photon cannot carry an angular momentum of 2, the $J = \pm 2$ states are optically dark, while the states with $J = \pm 1$ and 0 can be either dark or bright. The inset in Figure 1 shows schematically the exciton fine structure associated with 1S–1S transition for the CdSe QD.

By comparing Figure 2 with Figure 3, it is seen that the size dependence of exciton spin relaxation dynamics shows two decaying processes with very different time scales; a fast component with time constant of several picoseconds and a slow one with hundreds of picoseconds even to the nanoseconds time scale. For the large CdSe QD (for example, $d = 5.2$ nm), the fast component dominates the decay process, and the slow process is almost undetectable. The spin relaxation dynamics can be well-fitted with single exponential decay. When particle size decreases (for example, in the cases of 4.0 and 2.4 nm CdSe QDs shown in Figure 3), both fast and slow decaying processes are clearly observable. Photoexcitation of CdSe QDs with circular polarization of laser pulses, the excitons with particular spin alignment are populated in the optically active states of $J = \pm 1$ depending on the helicity of the light. Exciton spin relaxation occurs through interlevel and/or

intralevel transition among the band-edge exciton fine structures. We attribute the fast relaxation observed in the experiments to the interlevel exciton transition in which the process of the hole spin is flipped, while electron spin is conserved. This process can be treated as the exciton transition from the states, $(S_e S_h)_{\pm 1/2, \mp 3/2}$ (with $J = \mp 1$), to the states $(S_e S_h)_{\pm 1/2, \pm 3/2}$ (with $J = \pm 2$).³⁵ These processes without electron spin flip are much more probable than those with electron spin flip. The hundreds of picoseconds slow relaxation can be attributed to the intralevel exciton transition, which is corresponding to exciton transition from the states $(S_e S_h)_{\pm 1/2, \mp 3/2}$ ($J = \mp 1$) to the states $(S_e S_h)_{\mp 1/2, \pm 3/2}$ ($J = \pm 1$). This process requests that both hole and electron flip their spins, so it takes much longer time to complete this transition than the process of hole spin flip.^{28,36}

By using cross-polarized heterodyned third-order transient grating (CPH-3TG), the Scholes' group investigated the size and shape dependence of exciton fine structure relaxation in colloidal CdSe QDs, and the hole spin flip rate was found to be R^{-4} size dependence, where R is the diameter of the QD size.^{14,26,34} In fact, by using a Fermi golden rule rate expression, the exciton spin flip rate associated with $J = +1(-1)$ to $J = -2(+2)$ (corresponding to hole spin flip) can be expressed as

$$k_s \approx |M|^2 \rho \quad (1)$$

where ρ is the density of final states, and M is the matrix element for $J = \pm 1$ to $J = \mp 2$ transition. As a result of the Dresselhaus effect, M scales as $1/a^2$, with a , the exciton radius, and therefore, k_s (inversely proportional to spin lifetime, τ_s , i.e., $k_s \propto 1/\tau_s$) scales $1/a^4$ or R^{-4} for a strongly confined system.³⁴ It is seen from Figure 4 that the fast spin relaxation times are

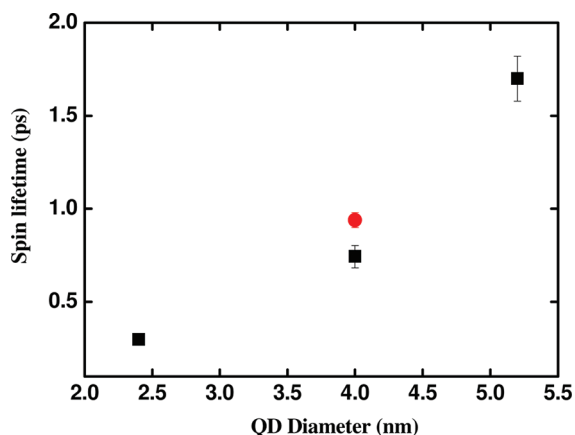


Figure 4. Fast spin relaxation time as a function of diameter of QD for both CdSe core (square) and CdSe/ZnS core-shell (filled dot) structures.

determined to be about 0.30, 0.74, and 1.80 ps for 2.4, 4.0, and 5.2 nm CdSe core QDs according to the biexponential fit to the experimental data, which is qualitatively in agreement with the prediction of eq 1 and also consistent with the reports in the literature.^{26,34} By employing the polarization-resolved pump-probe method, Nemec et al.²² investigated the spin dynamics of quasispherical-shaped CdS QDs embedded into glass matrix. Exciton spin relaxation with two pathways with time constants of several picoseconds and nanoseconds time scale was observed, and they assigned the fast spin relaxation as the hole spin flip, while the electron spin is conserved. A

mechanism called two-LO-phonon assisted hole spin flip was proposed, in which one LO-phonon is absorbed and the other LO-phonon is emitted.^{26,28}

Figure 2d shows the photon energy dependence of spin relaxation in the 5.2 nm CdSe QDs. By detuning the excitation energy across the lowest exciton peak absorption, it is seen that when photon energy is decreased, on the one hand, CdSe QDs with relatively large size can be excited, which results in the relative longer spin relaxation time; on the other hand, with low pump energy, only the lower lying states in CdSe QDs are excited, which can exclude the contribution from light-hole transition. It is expected that the maximum degree of net spin polarization close to 100% can be reached due to the negligible light-hole transition. When the excitation energy is increased, the maximum degree of net spin polarization is less than 100% owing to the partial involvement of light-hole transition. Both cases lead to the relatively longer spin relaxation time with increasing excitation wavelength as shown in Figure 2d.

With decreasing the size of CdSe QDs, the exciton spin relaxation shows two relaxation pathways with significantly different time scales. As discussed above, the fast component comes from the hole spin flip, which shows strong particle size dependence, while the slow component with time constant of hundreds of picoseconds to nanoseconds time scale is associated with the electron spin flip, which is corresponding to the exciton transition from states with $J = -1(+1)$ to states with $J = +1(-1)$. By comparing the spin relaxation with different sizes of CdSe QDs, it is seen that the slow component is also strongly dependent on the particle size: the fast relaxation component plays a predominant role for the exciton spin relaxation process, and the slow one is almost undetectable in the 5.2 nm CdSe QD. Both the fast and slow relaxation components play equal important roles for the exciton spin relaxation in smaller CdSe QDs with diameters of 4.0 and 2.4 nm. It is also seen that the amplitude of the slow relaxation component plays a more and more important role when the particle size decreases. It is believed that the slow relaxation associated with electron spin flip is driven by the electron–hole exchange interaction.²³ The exchange interaction is scaled as $1/R^3$ with the radius R of the spherical QD,^{4,37} which can be greatly enhanced by confining electron and hole into a small space in a QD. Therefore, a larger exchange interaction is expected for a smaller QD size, and vice versa. That is why we did not observe the slow relaxation in 5.2 nm CdSe QDs, but the process is clearly observed in 4.0 nm and 2.4 nm CdSe QDs. As proposed by Nemec,²⁸ although the exchange interaction in CdSe is relatively weak, this interaction in combination with the exciton–phonon interaction can provide an effective channel for exciton spin relaxation processes, in which electron spin flip occurs.

As discussed above, there are two mechanisms that dominate the exciton spin flip process: one is a direct (or say single-step) spin flip between the $J = \pm 1$ exciton states; the other is an indirect spin flip in which electron and hole flip their spin independently. It is usually thought that the direct spin flip process is driven by the long-range term of the electron–hole exchange interaction, and the indirect spin flip is governed by strong spin–orbit coupling in QDs.^{23,29,30} In spherical CdSe QDs with larger particle size, electron–hole exchange interaction is weak so that the spin–orbit coupling dominates the spin relaxation process. As a result, the indirect spin flip via the $J = \pm 2$ dark states is a predominate pathway for exciton spin relaxation. In small size CdSe QDs, direct spin flip dominates

the exciton spin relaxation process owing to relatively large electron–hole exchange interaction.

5. SUMMARIES AND CONCLUSIONS

In conclusion, by employing polarized pump–probe spectroscopy, we investigated the exciton spin relaxation in colloidal CdSe QDs with quasishperical shape. Our experimental results demonstrate that exciton spin relaxation among the exciton fine structure states are strongly affected by the particle size. The exciton spin relaxation shows a single exponential decay for a large size of CdSe QD, the relaxation is believed to be associated with the hole spin flip, $J = \pm 1 \leftrightarrow \mp 2$ transition. For a small size of QD, the exciton spin relaxations show biexponential decay, the fast one with a typical time constant of several picoseconds, and a slow one with hundreds of picoseconds to nanoseconds time scale. The slow relaxation is attributed to the intralevel exciton transition, $J = \pm 1 \leftrightarrow \mp 1$ transition. Both fast and slow relaxation show strong particle size dependence.

AUTHOR INFORMATION

Corresponding Author

*E-mail: ghma@staff.shu.edu.cn.

Notes

The authors declare no competing financial interest.

ACKNOWLEDGMENTS

This research is supported by National Natural Science Foundation of China (11174195) and Science and Technology Commission of Shanghai municipal (09530501100).

REFERENCES

- (1) Gupta, J. A.; Knobel, R.; Samarth, N.; Awschalom, D. D. *Science* **2001**, *292*, 2458.
- (2) Ouyang, M.; Awschalom, D. D. *Science* **2003**, *301*, 1074.
- (3) Shelykh, I. A.; Kavokin, A. V.; Rubo, Y. G.; Liew, T. C. H.; Malpuech, G. *Semicond. Sci. Technol.* **2010**, *25*, 103001.
- (4) Tong, H.; Wu, M. W. *Phys. Rev. B* **2011**, *83*, 235323.
- (5) Gupta, J. A.; Awschalom, D. D.; Peng, X.; Alivisatos, A. P. *Phys. Rev. B* **1999**, *59*, R10421.
- (6) Tartakovskii, A. I.; Cahill, J.; Makhonin, M. N.; Whittaker, D. M.; Wells, J.-P. R.; Fox, A. M.; Mowbray, D. J.; Skolnick, M. S.; Groom, K. M.; Steer, M. J.; Hopkinson, M. *Phys. Rev. Lett.* **2004**, *93*, 057401.
- (7) Nair, P. S.; Fritz, K. P.; Scholes, G. D. *Chem. Commun.* **2004**, 47, 2084.
- (8) Yu, W. W.; Qu, L. H.; Guo, W. Z.; Peng, X. *Chem. Mater.* **2003**, *15*, 2854.
- (9) Brus, L. E. *J. Chem. Phys.* **1984**, *80*, 4403.
- (10) Alivisatos, A. P. *Science* **1996**, *271*, 933.
- (11) Ellingson, R. J.; Beard, M. C.; Johnson, J. C.; Yu, P.; Micic, O. I.; Nozik, A. J.; Shabaev, A.; Afros, A. L. *Nano Lett.* **2005**, *5*, 865.
- (12) Norris, D. J.; Bawendi, M. G. *Phys. Rev. B* **1996**, *53*, 16338.
- (13) Huynh, W. U.; Dittmer, J. J.; Alivisatos, A. P. *Science* **2002**, *295*, 2425.
- (14) Wong, C. Y.; Kim, J.; Nair, P. S.; Nagy, M. C.; Scholes, G. D. *J. Phys. Chem. C* **2009**, *113*, 795.
- (15) He, J.; Lo, S. S.; Kim, J.; Scholes, G. D. *Nano Lett.* **2008**, *8*, 4007.
- (16) Jiang, J. H.; Zhou, Y.; Korn, T.; Schüller, C.; Wu, M. W. *Phys. Rev. B* **2009**, *79*, 155201.
- (17) Takagahara, T. *Phys. Rev. B* **1993**, *47*, 4569.
- (18) Kusrayev, Y. G. *Semicond. Sci. Technol.* **2008**, *23*, 114013.
- (19) Lloyd, S.; Braunstein, S. L. *Phys. Rev. Lett.* **1999**, *82*, 1784.
- (20) Poggio, M.; Steeves, G. M.; Myers, R. C.; Stern, N. P.; Gossard, A. C.; Awschalom, D. D. *Phys. Rev. B* **2004**, *70*, R121305.
- (21) Scholes, G. D. *J. Chem. Phys.* **2004**, *121*, 10104.
- (22) Horodyská, P.; Němec, P.; Sprinzl, D.; Malý, P.; Gladilin, V. N.; Devreese, J. T. *Phys. Rev. B* **2010**, *81*, 045301.
- (23) Kim, J.; Wong, C. Y.; Nair, P. S.; Fritz, K. P.; Kumar, S.; Scholes, G. D. *J. Phys. Chem. B* **2006**, *110*, 25371.
- (24) Scholes, G. D.; Kim, J.; Wong, C. Y.; Huxter, V. M.; Nair, P. S.; Fritz, K. P.; Kumar, S. *Nano Lett.* **2006**, *6*, 1765.
- (25) He, J.; Zhong, H. Z.; Scholes, G. D. *Phys. Rev. Lett.* **2010**, *105*, 046601.
- (26) Kim, J.; Wong, C. Y.; Scholes, G. D. *Acc. Chem. Res.* **2009**, *42*, 1037–1046.
- (27) Efros, A. L.; Rosen, M.; Kuno, M.; Nirmal, M.; Norris, D. J.; Bawendi, M. *Phys. Rev. B* **1996**, *54*, 4843.
- (28) Nahálková, P.; Sprinzl, D.; Malý, P.; Němec, P.; Gladilin, V. N.; Devreese, J. T. *Phys. Rev. B* **2007**, *75*, 113306.
- (29) Vinattieri, A.; Shah, J.; Damen, T. C.; Kim, D. S.; Pfeiffer, L. N.; Maialle, M. Z.; Sham, L. J. *Phys. Rev. B* **1994**, *50*, 10868.
- (30) Bir, G. L.; Pikus, G. E. *Sov. Phys. JEPT* **1971**, *33*, 108.
- (31) Ma, H.; Jin, Z. M.; Ma, G. H.; Liu, W. M.; Tang, S. H. *Appl. Phys. Lett.* **2009**, *94*, 241112.
- (32) Ma, H.; Jin, Z. M.; Wang, L.; Ma, G. H. *J. Appl. Phys.* **2011**, *109*, 023105.
- (33) Ma, H.; Ma, G. H.; Wang, W. J.; Gao, X. X.; Ma, H. L. *Chin. Phys. B* **2008**, *17*, 1280.
- (34) Huxter, V. M.; Kim, J.; Lo, S. S.; Lee, A.; Nair, P. S.; Scholes, G. D. *Chem. Phys. Lett.* **2010**, *491*, 187.
- (35) Němec, P.; Nahálková, P.; Sprinzl, D.; Malý, P.; Gladilin, V. N.; Devreese, J. T. *Phys. Status Solidi C* **2006**, *3*, 4291.
- (36) Sprinzl, D.; Nahálková, P.; Devreese, J. T.; Gladilin, V. N.; Malý, P.; Němec, P. *Phys. Status Solidi C* **2006**, *3*, 870.
- (37) Kadantsev, E.; Hawrylak, P. *Phys. Rev. B* **2010**, *81*, 045311.